Friction **4**(4): 359–368 (2016)
DOI 10.1007/s40544-016-0132-8
ISSN 2223-7690
CN 10-1237/TH
RESEARCH ARTICLE

Behaviors of a micro oil droplet in an EHL contact

Xinming LI[1], **Feng GUO**[1,*], **Shaopeng WANG**[1], **Chenglong LIU**[1], **Wenzhong WANG**[2]

[1] *School of Mechanical Engineering, Qingdao University of Technology, Qingdao 266520, China*

[2] *School of Mechanical Engineering, Beijing Institute of Technology, Beijing 100081, China*

Received: 24 August 2016 / Revised: 28 October 2016 / Accepted: 16 November 2016

Abstract: Oil–air lubrication supplies lubricants in the form of droplets to elastohydrodynamic lubrication (EHL) contacts, such as those in high-speed spindle bearings. However, there is a paucity of information related to understanding the lubrication behaviors of oil droplets within EHL contacts. In this study, behaviors of lubricant droplets, in terms of spreading around a static contact as well as passing through a rolling contact, were studied with an optical ball-on-disk EHL test rig. Influences of oil droplet size, viscosity, and surface tension on droplet spreading were examined. Lubricating film formation was also investigated when droplets traveled through the EHL contact region. The results indicated that droplet size and running speed significantly influenced film profiles. With increasing entrainment speeds, a small droplet passed through the contact without spreading and generated films with a significant depression in the central contact region.

Keywords: oil droplet; spreading; elastohydrodynamic lubrication; optical interferometry

1 Introduction

Recently, significant progress was achieved in lubrication approaches of machine components, such as bearings and gears, operating under high-speed conditions. Grease lubrication is typically preferred due to the ease of maintenance and lubricant retention in the components. However, the running speeds are limited for bearings due to overheating and grease deterioration. An oil-jet lubrication method is often chosen for high-speed and heavy-duty components, and the consumption of large amounts of oil is involved in removing heat from churning loss and in avoiding lubricant starvation. An oil-mist technique is also used to lubricate rubbing surfaces, in which oil droplets (with sizes in the range of 1–5 micrometers) are brought to lubricated areas. However, the oil-mist technique can cause environment hazards, and the oil cannot be fully converted to the desired mist drops by the lubrication system. Alternatively, oil–air lubrication was presented as an attractive approach to efficient lubrication through the idea of lubricant supply by means of small amounts over frequent intervals [1]. In oil–air lubrication, oil metered by the distributor is driven by compressed air along the walls of a transportation tube in streaks and fed at the terminating nozzle to the bearings as refined oil droplets. This is superior to other lubrication methods due to accurate oil quantity regulation, suppression of temperature increases, dirt ingress prevention, reduction in lubricant consumption, and environment-friendliness. Subsequently, this precise and effective lubrication method is an optimal choice for high-speed spindles, gear transmission [2], chain conveyors, and metallurgical equipment [3].

For several decades, previous studies examined oil–air lubrication and were performed directly with respect to industrial practices. This was particularly true for bearings of high-speed spindles. Experimental studies mostly focused on evaluating oil–air working parameters by investigating temperature increases, such as preloads, oil quantities, compressed air flow rates, rotating speeds [4], tube lengths, time intervals [5], oil viscosity, and nozzle types [6]. The main purpose

* Corresponding author: Feng GUO.
E-mail: mefguo@163.com

Nomenclature

a	diameter of Hertz contact, m	t	time, s
D	width of spreading layer, m	T	time ratio
D_{ini}	initial droplet diameter, m	t_a	actual lubrication time, s
h_{layer}	thickness of spreading droplet layer, m	t_n	nominal lubrication time, s
K	constant	u_e	entrainment speed, m/s
L_s	distance between the droplet center and the contact center, m	u_{sp}	spreading speed, m/s
		v	velocity of liquid, m/s
p	pressure, Pa	V	volume of droplet, m^3
ΔP_L	left side pressure of liquid, Pa	v'	average velocity of liquid, m/s
ΔP_R	right side pressure of liquid, Pa	w	applied load, N
ΔP	capillary pressure, Pa	x, y, z	coordinates, m
R	radius of droplet, m	γ	surface tension, N/m
R_L	left side curvature of the lubricant layer, m	η	viscosity, Pa·s
R_R	right side curvature of the lubricant layer, m	θ	contact angle, degree

of these studies involved finding optimal working parameters for specific oil–air lubrication systems [7]. However, there is a shortage of information related to the workings of an oil droplet in building a lubrication film inside bearings. As is widely known, the main lubrication mechanism in bearings involves elastohydrodynamic lubrication (EHL) in which film formation is determined mainly by the lubricant supply conditions outside the contact region [8]. Thus, oil droplet size, distribution, and spreading behaviors on the race surfaces can determine oil supply conditions out of the contact region and consequently affect EHL films [9].

A project was undertaken to address the aforementioned issues. The preliminary step included an optical EHL test rig that was used to investigate the spreading behaviors of an oil droplet in contact with the bounding surfaces of a stationary ball-on-disc contact, and this could occur when oil/air is pre-supplied to tribo-pairs prior to operation. However, in the present laboratory tests, oil droplets were arranged artificially on the disc surfaces as opposed to being generated from an oil–air system. Under pure rolling conditions, a droplet was entrained into the contact and the dynamic film formation was recorded. The obtained results were beneficial and contributed to a better understanding of the film formation in EHL with oil droplets.

2 Experimental set up

The experiments were performed with an optical EHL test rig. Figure 1 schematically shows the test rig used and the experimental scheme. A steel ball was loaded against a glass disc, and the loaded side of the glass disc was coated with a Cr layer as a beam splitter for interferometry. The highly polished steel ball had a diameter of 25.4 mm and a roughness of R_a = 10 nm. The glass disc was driven by a servomotor, and the steel ball was then automatically rotated to achieve a pure rolling running condition.

As shown in Fig. 2, prior to the experiments, a series of oil droplets were elaborately arranged on the glass disc by micropipettors. Figure 2(a) shows a side view of the droplets in which θ denotes the contact angle

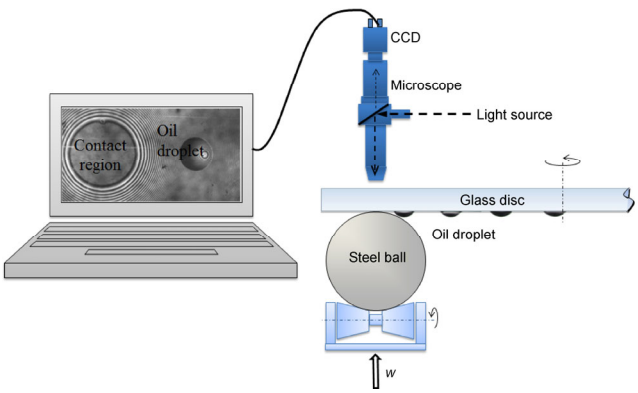

Fig. 1 Illustration of the test rig and the test scheme.

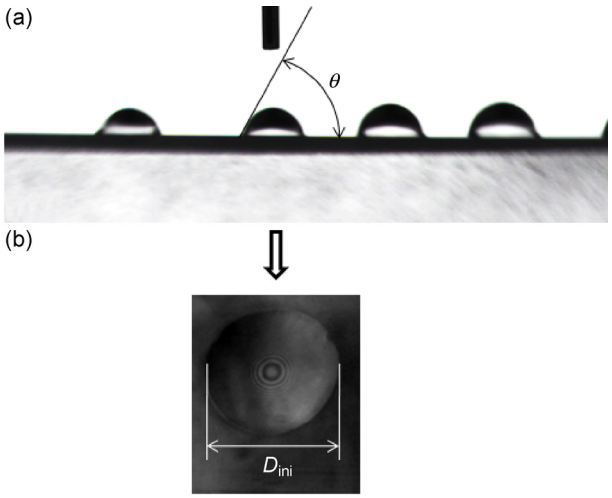

Fig. 2 Oil droplets arrangement and their shape (PAO100, Cr surface): (a) side view; (b) top view.

that was obtained by a contact angle goniometer. Figure 2(b) shows the top view of a droplet measured from the optical EHL test rig in which the droplet initial diameter D_{ini} could be readily measured. Theoretically, given the assumption of a constant contact angle and a regular spherical cap, the volume of the droplet could be roughly calculated by D_{ini}. However, the measurement indicated that when the droplet volume was downsized to picoliter scales (or D_{ini} less than 500 μm), the contact angle θ could increase with decrease in the droplet size. A large droplet volume presents a large D_{ini}. Hence, in this study, the droplet diameter D_{ini} was used to represent the droplet size. In each experiment, the position of the steel ball was adjusted to accommodate the droplet in the central rolling track. The film profiles were reconstructed via a multi-beam intensity-based method [10].

Experiments were performed at an ambient temperature of 20 ± 1 ˚C. Different types of lubricants were employed and their properties are listed in Table 1.

Table 1 Properties of the lubricants used in the experiments.

Lubricant	Viscosity (Pa·s@20 ˚C)	Density (kg·m^{-3}@ 20 ˚C)	Refractive index
PAO4	0.025	0.819	1.456
PAO8	0.049	0.833	1.463
PAO100	1.800	0.847	1.520
Silicone 201-1000	1.000	0.975	1.405
5P4E	5.410	1.205	1.630

3 Results and discussion

3.1 Spreading of oil droplets under static contacts

In this section, the spreading of an oil droplet around a stationary ball-on-disc contact was measured. This spreading may occur when an oil droplet enters the bearings prior to the operation and subsequently influences the lubrication behaviors during the start-up process.

In each experiment, the droplet was transported to a position close to the contact region at an ultralow speed (approximately 5 μm/s). This type of a low speed was obtained via a precision reducer. The motion stopped immediately when the droplet started to contact the ball surface.

Figure 3 shows the typical spreading process of an oil droplet around the peripheral gap of a Hertzian contact. Image A indicates the initial stage in which the disc rotated at a very slow speed. In image B, the disc was stationary and the droplet just entered into contact with the ball surface, and thus, deformation on the droplet could be observed. The deformed droplet indicated an asymmetrical liquid bridge within the gap, which induced the resultant capillary force that transported the liquid toward the contact region. It is interesting to note that the deformed part separated itself from the original droplet as shown in images C and D, thereby indicating that the capillary force was sufficiently strong to overcome the cohesion inside the droplet. Following this, the separated liquid began to spread around the contact region (images E and F), and the peripheral gap outside the contact area was symmetrically filled. As shown in Fig. 3, only part of the droplet filled the peripheral gap of the contact and directly affected the film formation of the contact pair start-up.

The droplet spreading could be interpreted in terms of a replenishment mechanism [11, 12]. The replenishment was divided into “out-of contact” reflow and “in-contact” reflow [12]. The “out-of contact” reflow occurred in the lubricant track after it emerged from the contact wake, and this was influenced by surface tension (or centrifugal force) and the oil viscosity. The “in-contact” mechanism describes lubricant reflow close to the contact that contributed to replenishment in the vicinity of the contact due to the local capillary

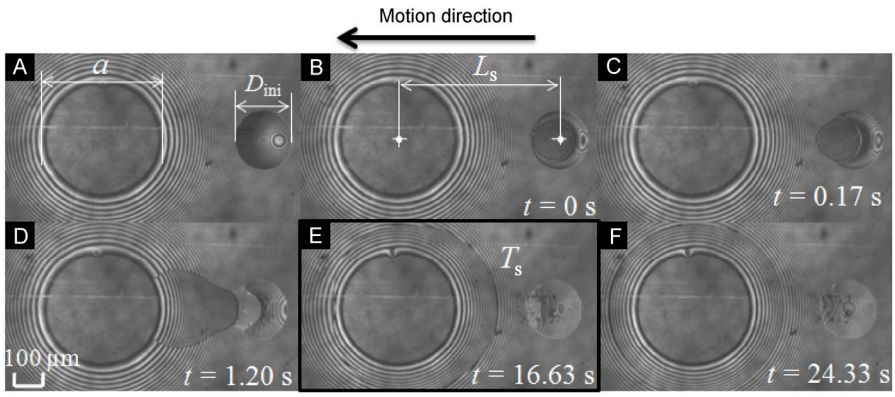

A Initial state; B Droplet deformation; C Separating; D Spreading; E Initial surounding; F Total surrounding

Fig. 3 Spreading process of a micro-oil droplet, PAO100, w = 54 N, D_{ini} = 212 μm.

force. Evidently, the movement and spreading of the deformation part were induced by the capillary force, which corresponded to the "in-contact" reflow mechanism. In the process, the residual part regained a hemisphere shape due to the surface tension.

In order to describe the spreading process, the parameters are defined as shown in Fig. 3, where a denotes the diameter of the Hertz contact, and D_{ini} denotes the initial diameter of the droplet as also defined in Fig. 2. Additionally, L_s denotes the distance between the contact center and the droplet center at the time when the droplet started to contact the ball surface. At the instant shown in Image E, the spreading layer initially enclosed the whole contact. The motion time of the separated part from Image B to E was defined as the spreading time (denoted as T_s). The average spreading speed can be defined as follows:

$$u_{sp} = \frac{L_s}{T_s} \tag{1}$$

Specifically, this is a non-linear process for a droplet spread. In terms of a simplified analysis, the nominal speed u_{sp} can be used to evaluate the droplet spreading level.

Figure 4 illustrates the influence of the initial droplet size (denoted as D_{ini}) on the average droplet spreading speed. Evidently, a large droplet resulted in a higher spreading velocity. The results can be explained in terms of Fig. 5 that schematically depicts the spreading of the liquid due to Laplace pressure difference. This is expressed as follows:

$$\Delta P = \gamma\left(\frac{1}{R_R} - \frac{1}{R_L}\right) \tag{2}$$

where γ denotes the surface tension of the liquid, R_L and R_R denote the radius of the curvature at the right and left end surfaces, respectively, of the lubricant slug (1-Dimensional for simplification). It is obvious that $R_L > R_R$, and this implies that the net pressure difference in Eq. (2) drives the lubricant to move towards the converging gap, and thus spreads circumferentially around the contact. However, the difference between R_L and R_R reduced as spreading proceeded, which indicated a decrease in ΔP, and therefore, resulted in slow spreading. Therefore, if a larger droplet began spreading at position 1 (Fig. 5(a)) and occupied a larger space, then the spreading velocity was enhanced by a larger ΔP. In contrast, the smaller droplet remained initially at position 2 (Fig. 6(b)) and occupied a smaller

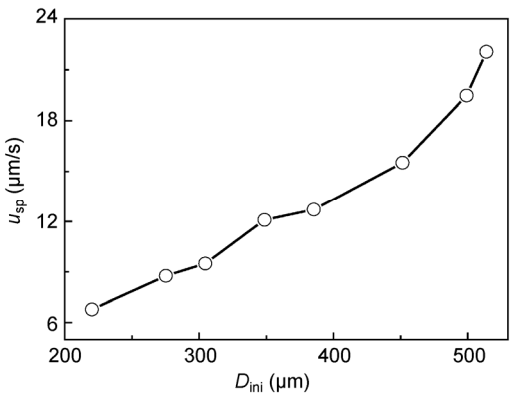

Fig. 4 Influence of droplet size on spreading velocity, PAO100, w = 42 N.

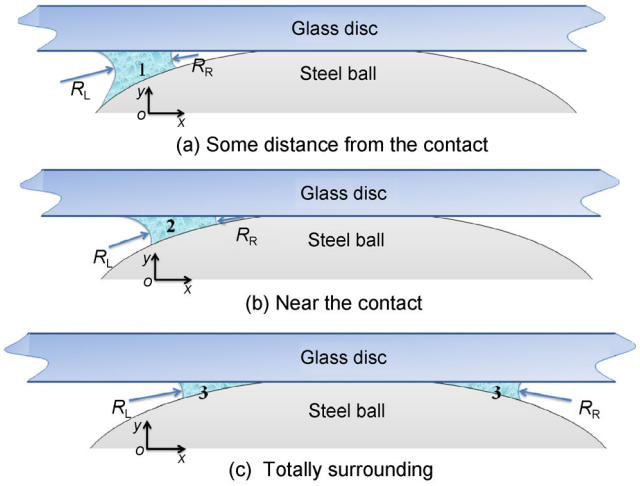

Fig. 5 Spread of the separated part due to capillary pressure.

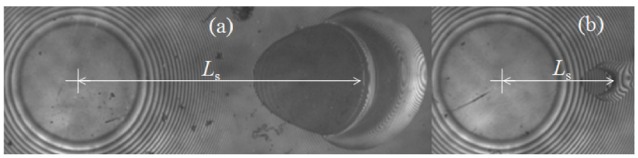

Fig. 6 Initial spreading positions of large and small droplets, (a) D_{ini} = 452 μm; (b) D_{ini} = 142 μm, PAO100, w = 48 N.

space, which produced a smaller initial ΔP and correspondingly a lower spreading speed. As shown in Fig. 6, it was found that even the spreading distance of a larger droplet is longer than that of the small one, it still spreads faster. For all the droplets, they surround the contact region at last and build a capillary bridge with $\Delta P = 0$.

Figure 7 compares the spreading velocities (denoted as u_{sp}) of two lubricants, namely PAO4 and PAO8, with different viscosities. In a manner similar to Fig. 4,

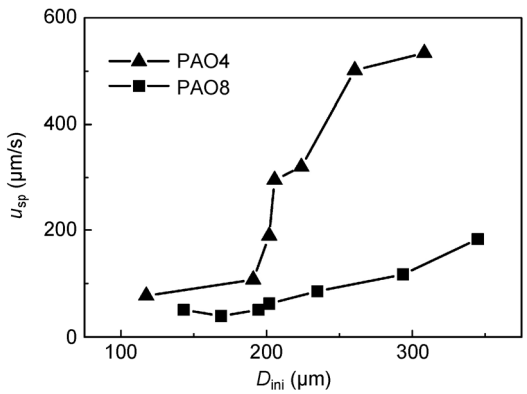

Fig. 7 Influence of viscosity on spreading velocity, w = 30 N, D_{ini} = 220 μm.

the spreading speed increased with droplet size but the values were considerably higher than those in Fig. 4. Evidently, the lubricant with lower viscosity was easier to spread. Given the thin liquid film spreading as shown in Fig. 5, for an infinitesimal liquid element, there exists the following relation:

$$\frac{\partial p}{\partial x} = \eta \frac{\partial^2 v}{\partial y^2} \tag{3}$$

where p denotes pressure, v denotes speed along the x direction, and η denotes lubricant viscosity. By integrating this equation, an average of the lubricant velocity across the film can be expressed as follows:

$$v' = \frac{\int_0^{h_{layer}} v \mathrm{d}y}{h_{layer}} = \frac{h_{layer}^2}{12\eta} \frac{\partial p}{\partial x} \tag{4}$$

where h_{layer} denotes thickness of spreading layer/gap height. As shown in Eq. (4), the lubricant average speed was inversely proportional to the viscosity. The analysis corresponded to results shown in Fig. 7.

Figure 8 shows the droplet spreading process of silicone 201-1000. Silicone oils have very low surface tension and good affinity to solid surfaces. It was observed that the occurrence of the droplet deformation (or contact with the ball) was quite close to the edge of the contact region due to a small contact angle of the glass disc. In contrast to the process in Fig. 3 of PAO oils, the silicone oil droplet was split several times, such as the first splitting in Image C followed by the second splitting in Image D. Finally, the split parts recombined, and a meniscus film layer was formed to enclose the contact region.

3.2 Droplet passing through a rolling contact

Figure 9 presents a droplet passing through the contact region under pure rolling conditions. The applied speed and load corresponded to 0.37 mm/s and 30 N, respectively. The initial size corresponded to D_{ini} = 1,020 μm. The magnification of the microscope was adjusted to a low level to observe the whole droplet. Image A shows the initial size of the droplet that was considerably larger in radius than the Hertz contact. Additionally, u_e corresponded to the entrainment speed. During the passage of the droplet through the

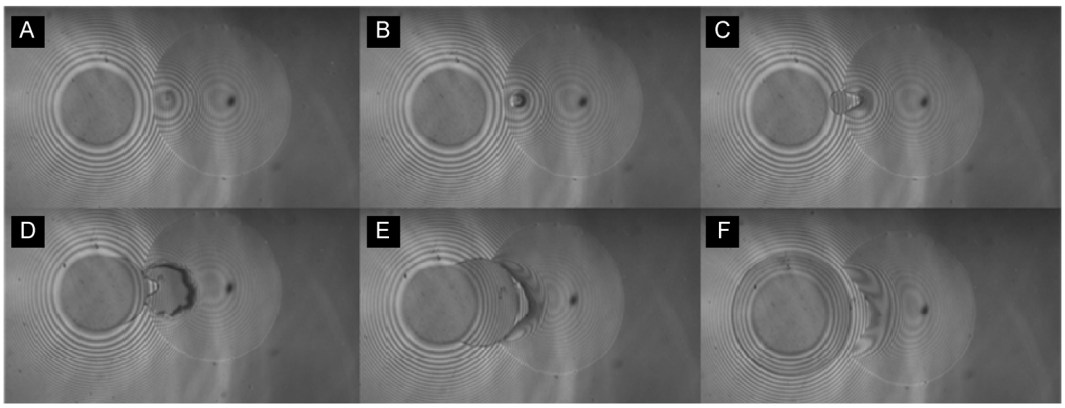

A Droplet deformation; B and C Spreading; D and E Partial surrounding; F Total surrounding

Fig. 8 Droplet spreading of silicone 201-1000, w = 30 N, D_{ini} = 680 μm.

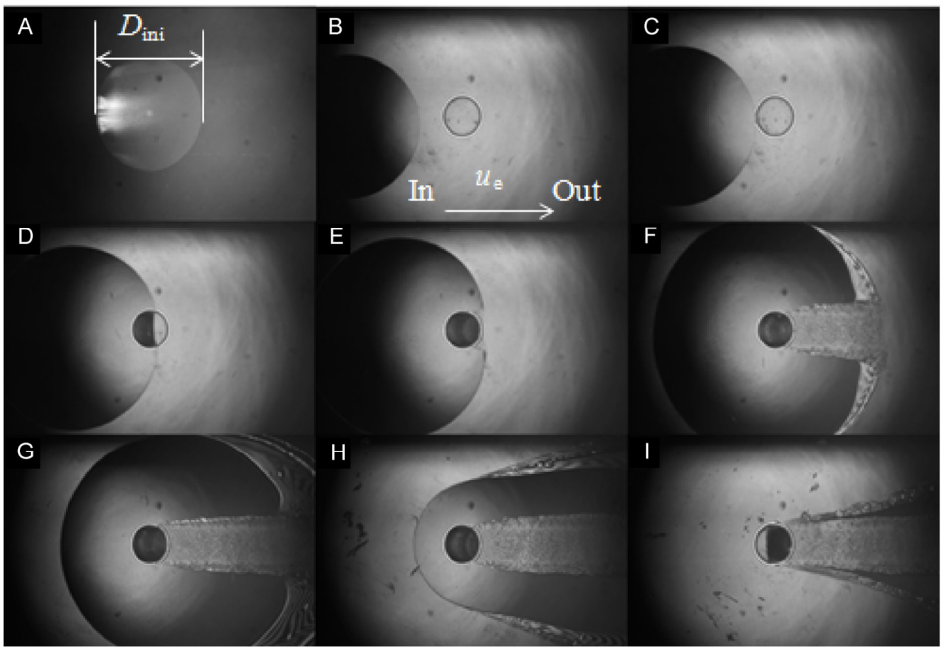

A Initial size; B Approaching; C Arrial of contact edge; D~G Passing; H and I Leaving

Fig. 9 Droplet passing through the contact region, 5P4E, u_e = 0.37 mm/s, w = 30 N, D_{ini} = 1,020 μm.

contact region, it was observed that the base radius of the droplet increased and reached its maximum in image F wherein the droplet center and contact center nearly overlapped. This enlarged shape could be attributed to the squeezing experienced when the droplet approached the gap with decreasing size and the spread due to the surface tension. As shown in image E, the cavitation appeared at the moment when the lubricant film started to leave the contact region and entered a diverging gap. As shown in image F, the contact pair split the droplet apart, and further cavitation occurred at the film front near the central outlet at which there was more abrupt gap divergence. Additionally, no typical EHL film shape was observed due to the very low film thickness under low speeds.

As described above, the change in the droplet shape (or increase in base radius) as shown in Fig. 9 indicated spreading and squeezing due to the convergence of the gap at the inlet. In order to characterize the influence of droplet spreading and squeezing on lubrication, a nominal lubrication time (denoted as t_n) and an actual lubrication time (denoted as t_a) were defined. As shown in Fig. 10, if a droplet passed through the contact region without changing its initial

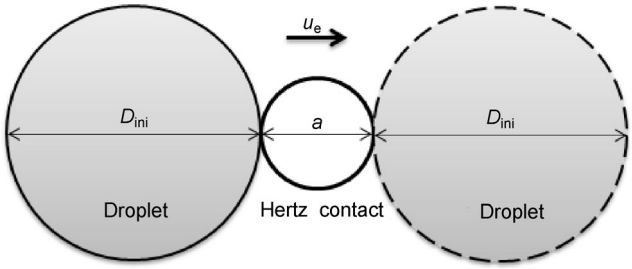

Fig. 10 Definition of nominal lubrication time.

diameter (denoted as D_{ini}), then the nominal lubrication time can be expressed as follows:

$$t_n = \frac{(a + D_{ini})}{u_e} \tag{5}$$

The actual lubrication time t_a was the time measured from the moment the droplet touched the contact edge until the lubricant left the contact region completely. A lubrication time ratio (denoted as T) can be further defined as follows:

$$T = \frac{t_a}{t_n} \tag{6}$$

T denotes the effects of spreading and squeezing on the duration of single droplet lubrication.

Figure 11 shows the variations of t_n, t_a, and T with entrainment speed. It was easily observed that the actual lubrication time considerably exceeded the nominal time. The difference was particularly significant in the low speed cases. The difference between t_a and t_n decreased with increase in the speed. The droplets

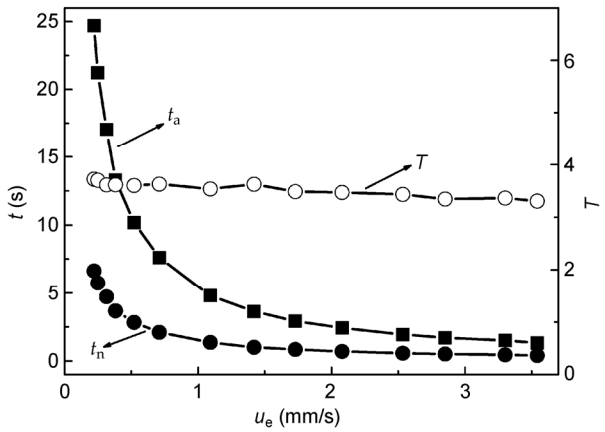

Fig. 11 Variations of t_n, t_a, and T with entrainment speed, 5P4E, w = 30 N, D_{ini} = 1020 μm.

had more time to spread when the speed was low. Furthermore, it was very interesting to note that T did not change significantly and was in the range of 3.5 and 3.8, which implied that spreading and squeezing effects played a role in extending the lubrication time in this speed range.

Figure 12 shows the lubricating film generation with a PAO100 droplet, u_e = 95.1 mm/s, w = 30 N, and D_{ini} = 274 μm. Due to the quick entrainment, a typical EHL film appeared when the droplet passed through the central contact. In a manner similar to the case in Fig. 9, the droplet shape enlarged when it entered the contact gap due to the spreading by surface force and squeezing, which in fact presented an improved lubricant supply. The spreading droplet and the generated lubricating film could cover the entire contact region. From images D to F, a full film was built with a classical EHL film shape. A starved film shape appeared in image G due to the absence of any further lubricant supply in the inlet region. Following this, the lubricating film gradually receded from the contact region. The corresponding film profiles are shown in Fig. 13, which illustrates the dynamic formation and recession of the EHL films. Figure 14 indicates the variations of central film thickness with respect to time. As shown in the figure, there was first an increase and then a decrease when the droplet entered and exited the contact region.

Figure 15 shows the observed film shapes with increase in entrainment speed or decreases in droplet size with PAO100. As shown in Fig. 15(a), the droplet size was smaller than that in Fig. 12. However, the droplet speed was higher, and the film indicated a shallow local depression, as opposed to a flat plateau, when the droplet passed through the central contact. At the inlet, given a small lubricant quantity or quick entrainment, the droplet spread due to the capillary force or squeezing was too limited to form a full lubricating film, and consequently it entered the contact in a manner similar to a "rigid body", and a local depression was formed on the solid surface. The liquid drop size corresponded to the largest in Fig. 15(a) and the smallest in Fig. 15(c). As shown in Fig. 15(c), only a partial area was separated by the lubricant film. In such cases, the variations of time ratio with droplet size are illustrated in Fig. 16. The magnitude

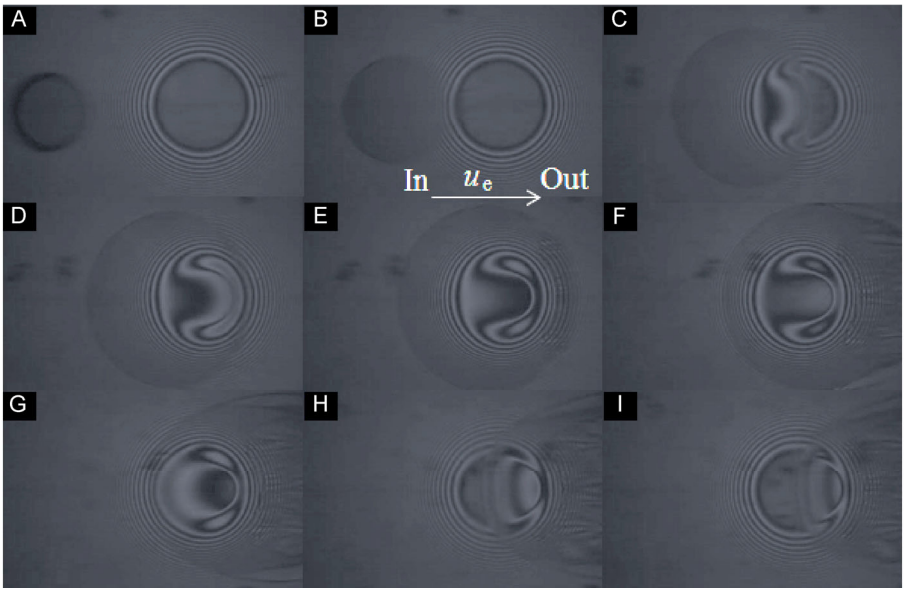

Fig. 12 Interferograms of droplet passing through the rolling contact, PAO100, u_e = 95.1 mm/s, w = 30 N, D_{ini} = 274 μm.

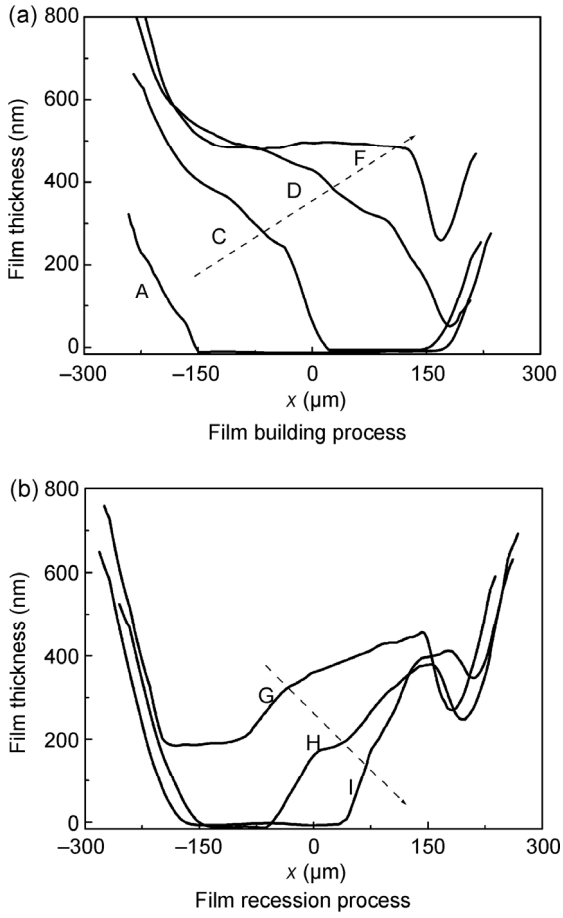

Fig. 13 Film profiles with droplet passing through the contact region, PAO100, u_e = 95.1 mm/s, w = 30 N, D_{ini} = 274 μm.

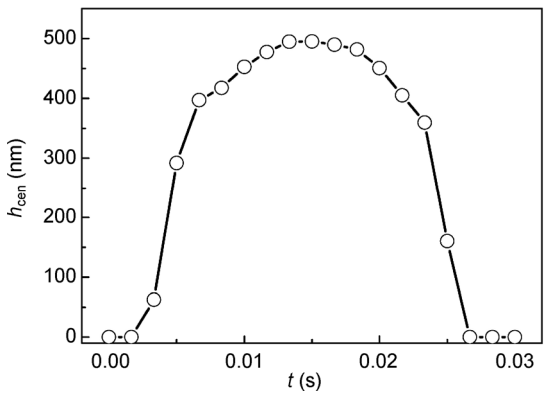

Fig. 14 Variations of central film thickness with time, PAO100, u_e = 95.1 mm/s, w = 30 N, D_{ini} = 274 μm.

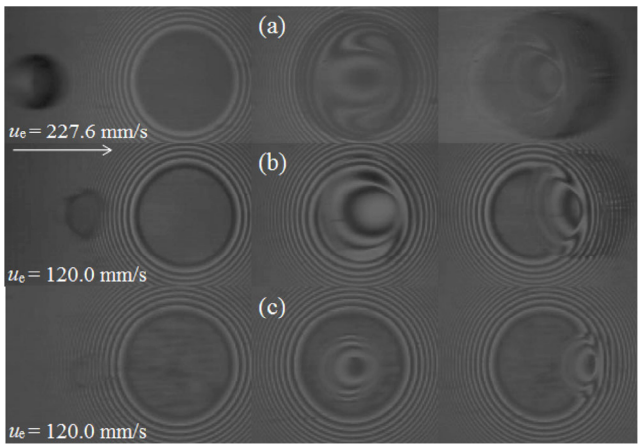

Fig. 15 Lubrication process with different dimple size and speed, PAO100: (a) D_{ini} = 187 μm; (b) D_{ini} = 143 μm; (c) D_{ini} = 87 μm, w = 30 N.

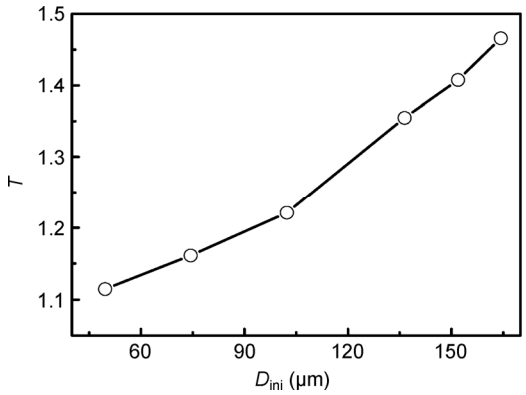

Fig. 16 Variations of time ratio T with initial droplet diameter D_{ini}, PAO100, u_e = 120.0 mm/s, w = 30 N.

of T was considerably lower than that in Fig. 11. The time ratio (denoted by T) decreased with decreases in droplet size. With respect to a limiting case, T could reach a value of 1 at which no spreading occurred.

As previously mentioned, the time ratio T essentially reflected spreading and squeezing effects on the duration of lubrication, that is, if the next droplet can catch up in time before the present droplet finishes lubrication, then a continuous lubrication can be maintained. Otherwise, discontinuous lubrication could occur.

4 Conclusions

In this study, EHL film generation behaviors of droplets under static and rolling ball-on-disk contacts were experimentally examined. The results can be summarized as follows:

1. When a lubricant droplet approached the convergent gap out of a static Hertz contact, it spread and filled the gap due to the capillary force. Droplets of large size and low viscosity were associated with high filling speeds.

2. The dynamic film building process of a droplet passing through a rolling contact was recorded. A time ratio (denoted by T) was defined to evaluate the effect of droplet spreading (by capillary force and squeezing) on the duration of lubrication. The results indicated that the spreading improved with higher values of T. The time ratio T decreased with increase in speed and viscosity and decrease in the droplet size.

3. With respect to a droplet of small size and high viscosity, there was insufficient droplet spreading at quick entrainment, and the contact region could not be fully lubricated and a dimple-shaped film occurred.

Acknowledgement

The authors would like to express their thanks to the financial supports from the Natural Science Foundation of China (No. 51405525), Doctoral Scientific Fund Project of the Ministry of Education of China (No. 20133721110002) and Outstanding Young Scientist in Shandong Province (No. BS2014ZZ004).

References

[1] Tret'yakov E I, Yurchenko N A**,** Lysyak A A. Improving oil-air lubrication systems. *Metallurgist* **48**(7–8): 414–416 (2004)

[2] Höhn B R, Michaelis K, Otto H P. Minimised gear lubrication by a minimum oil/air flow rate. *Wear* **266**(3–4): 461–467(2009)

[3] Dudorov E A, Ruzanov A I, Zhirkin Y V. Introducing an oil-air lubrication system at a continuous-casting machine. *Steel in Translation* **39**(4): 351–354 (2009)

[4] Jeng Y R, Gao C C. Investigation of the ball-bearing temperature rise under an oil-air lubrication system. *Proc Inst Mech Eng Part J: J Eng Tribol* **215**(2): 139–148 (2001)

[5] Wu C H, Kung Y T. A parametric study on oil/air lubrication of a high speed spindle. *Precis Eng* **29**(2): 162–167 (2005)

[6] Jiang S H, Mao H B. Investigation of the high speed rolling bearing temperature rise with oil-air lubrication. *ASME J Tribol* **133**(2): 021101 (2011)

[7] Moon J H, Lee H D, Kim S I. Lubrication characteristics analysis of an air-oil lubrication system using an experimental design method. *Int J Prec Eng Manuf* **14**(2): 289–297 (2013)

[8] Spikes H. Sixty years of EHL. *Lubr Sci* **18**(4): 265–291 (2006)
[9] Damiens B, Venner C H, Cann P M E, Lubrecht A A. Starvation lubrication of elliptical EHD contacts. *ASME J Tribol* **126**: 105–111 (2004)
[10] Guo F, Wong P L. A multi-beam intensity-based approach for thin lubricant film measurements in non-conformal contacts. *Proc Inst Mech Eng J Eng Tribol* **216**: 281–291 (2002)
[11] Pemberton J, Cameron A. A mechanism of fluid replenishment in elastohydrodynamic contacts. *Wear* **37**: 185–190 (1976)
[12] Jocord B, Pubilier F, Cann P M E, Lubrecht A A. An analysis of track replenishment mechanisms in the starved regime. In *Proceedings of the 25th Leeds-Lyon Symposium on Trib*, 1999: 483–492.
[13] Liu X, Guo D, Liu S, Xie G, Luo J. Interfacial dynamics and adhesion behaviors of water and oil droplets in confined geometry. *Langmuir* **30**: 7695–7702 (2014)

Feng GUO. He got his Ph.D. degree in mechanical engineering from the City University of Hong Kong in 2003. He is now employed as a full-time professor in Qingdao University of Technology. His main work is concentrated on fundamental research and university education in tribology. His research interests include numerical computation of liquid film lubrication, optical interferometry for lubricating film measurement, interfaces in tribology, and new lubrication techniques.

Xinming LI. He got his Ph.D. degree in School of Mechanical Engineering, Qingdao University of Technology in 2012. He is now employed as a full-time associate professor in Qingdao University of Technology. His recent research interests include bearing lubrication mechanisms, lubricant rheology, and lubrication approaches of machine elements.